Science & Justice 66 (2026) 101403

Contents lists available at ScienceDirect

Science & Justice

journal homepage: www.elsevier.com/locate/scijus

Lens correction techniques and their application in forensic photogrammetry

Kevin Gilmore [a,b], Geoffrey T. Desmoulin [a,*]

[a] GTD Scientific, Inc., Vancouver, Canada
[b] University of British Columbia Department of Biomedical Engineering, Vancouver, Canada

ARTICLE INFO

Keywords:
Lens distortion
Lens correction
Photogrammetry
Forensic investigation

ABSTRACT

In the field of forensics, digital media, such as images and videos, can become key pieces of evidence in any investigation. However, to correctly use images and videos for analysis and measurement, the images must be geometrically true. As such, it is essential to perform correction of the distortion of the images caused by the lens of the camera, as is recommended by forensic photography best practices and guidelines. In order to quantify the error associated with this correction, 3 techniques were compared: control point, straight-line, and manual lens correction. An idealized digital image was first created with no distortion, which was then distorted to 10 varying severities. Each resulting image was then corrected by each of the 3 techniques to attempt to remove the distortion. The level of distortion remaining was quantified by examining specific pixel locations before distortion and after correction. The results of the study found that the control point technique outperformed both others, with the manual technique outperforming the straight-line method. In regard to the application in forensics, the control point technique is the most accurate and also provides camera location information, and thus is the most suitable for use.

1. Introduction

In forensic investigations, all relevant data must be utilized to analyse the incident and draw conclusions, whether regarding injuries, the timeline of events, subject identity, or other such significant information. As such, information is obtained from various sources, including, but not limited to, medical reports, witness statements, scene forensics, and digital media recordings of the scene and incident. The digital data can be especially useful as it records an objective view of the incident and the site in question and can be used to both view the incident as it happened, track the timing of events, and provide a foundation for performing relevant measurements. However, recorded media, such as videos and photographs, suffer from certain drawbacks, such as not providing direct 3-dimensional information, or distortion of the image due to the camera's optical element misalignment, motion blur, and other artifacts [1]. In particular, lens distortion must be corrected for before the images or videos can be further used in analysis when geometric trueness is required, such as when performing measurements of the incident scene using the available digital media. The objective of this study is to inform investigators of the effectiveness, benefits, and drawbacks of various lens correction techniques, without the consideration of any specific further investigative measurements to allow for larger generalization of these results.

Lens distortion occurs due to, among other things, non-uniformity of the curvature of the lens used on the camera [1]. Typically, due to the nature of the lens, these distortions occur radially in two main forms, pincushion and barrel distortion [2,3]. In pincushion distortion, lines which are physically horizontal or vertical in the image will appear to bend inward toward the centre of the image, while the opposite is true for barrel distortion [2,3]. Aside from radial distortions, other forms of distortion may also occur due to the optical elements in a camera, though these are often less significant to the overall geometric correctness of the image [2]. When using physical cameras and lenses, more complex distortion patterns arising from a combination of the above sources, such as both barrel and pincushion distortion are also present, though these more complex situations will not be considered in this study [2,3]. As distortion affects the visual appearance and location of any points of interest in the image, measurements made with distorted images cannot be said to be 'true' and may be significantly errant [2–4]. In forensics, this type of measurement using a 2D image is often done to determine person of interest height [5,6], vehicle or other object position [7], crash and injury mechanics [8,9], and other such

* Corresponding author.
E-mail address: gtdesmoulin@gtdscientific.com (G.T. Desmoulin).

https://doi.org/10.1016/j.scijus.2026.101403
Received 26 June 2025; Received in revised form 30 January 2026; Accepted 2 February 2026
Available online 3 February 2026

measurements. As these measurements involve the use of photogrammetric techniques such as spatial resection [10,11], spatial intersection [12,13], and reverse projection [14], which require accurate determination of the source camera location and orientation and geometric trueness to the actual pictured physical scene, the need for image distortion correction remains a constant. This is especially true considering the common use of third-party, onsite recordings such as those from CCTV security cameras [15]. Guidelines regarding the use of image analysis and photogrammetry for forensic and investigative use stress the need to minimize and compensate for distortion arising from the camera [16–18].

Various forms of lens distortion correction techniques exist and require different supporting information to be applied correctly. These correction techniques include common control point, straight-line, and manual correction [6,19]. Moreover, various iterations of mathematical and numerical models and machine learning algorithms have been applied to characterize distortion caused by lenses and other artifacts to perform corrections [20–37]. This study will focus on commercially available lens correction methods which are available to forensic investigators.

Common control point lens correction involves using a known, geometrically true, 3D reference of what is captured in the image to correct for lens distortion [19]. This method can be used to both correct for lens distortion and solve for the camera's location and orientation, through a technique known as spatial resection [10,11,38,39]. These references can include anything in which known 3D points exist in reference to each other or the camera [39]. In the field of forensic investigations, this is generally produced through use of a LiDAR, other depth-sensing camera, or a terrestrial laser scanner used after-the-fact at the incident scene, providing scene geometry and information about the presence and location of objects or key features. To correct for lens distortion with this technique, visible points which are common to both the image and 3D reference are identified and paired so that the same feature in both is linked [38]. The corresponding pairs of chosen common points are then aligned either visually or mathematically, to provide the lowest cumulative point to point error. As the 3D reference is considered to be geometrically true, the image is then undistorted to reduce this error further until an optimal value is reached [38,39]. The resulting image is then considered to be lens corrected and the visual overlay between the image and true 3D reference can be viewed for confirmation. Given a perfect lens correction, all features and common points should perfectly align. Due to the nature of this technique, it is only viable if a geometrically true 3D reference of what is seen in the image can be used or created.

This technique inherently also defines the location of the camera used to take the 2D image relative to the 3D object or scan used to define the 3D control points. Therefore, in addition to solving camera parameters and correcting for lens distortion, this process also results in a virtual camera which has the same characteristics and relative position and orientation information as the physical camera which took the image [38].

Straight line lens correction is somewhat more direct; however, it does require that physically straight lines be captured in the image, in both sufficient length and number. Within the distorted image, lines are drawn to follow surfaces or features which are known to be geometrically straight in truth but curved in the image [6,19]. Once lines of sufficient length and number are defined, the image is undistorted to force these curved lines into straightening, thus correcting for the distortion of the image. Due to the need for physically straight surfaces to be clear in the image, the application of this process can be limited. For example, a video taken in a wooded area may be difficult to correct with this technique if no known straight lines appear in the scene. Moreover, lines which cover more of the image will result in better corrections.

Manual correction is inherently a procedure by which an expert manually warps an image until they reach their determination of the optimal level of correction, leaving some aspect of subjectivity in play. Various tools exist for this purpose, such as Adobe Photoshop, GIMP and PTLens, and the mechanism or mathematical model by which the correction occurs may differ in both usage and method. For example, some manual correction software may allow for more specific control of the image warping or may implement different mathematical models to generate the warped image for correction. Moreover, the use of different mathematical models does not only apply to manual correction, but to any correction software or program. The same image may be corrected for lens distortion differently in one software package compared to another, even if the same overall technique, such as straight-line correction, is used in both. While the increased level of subjectivity in the manual distortion correction technique does impact its credibility for forensic or legal applications, there is still a potential for usage. As previously mentioned, the control point and straight-line methods require a known 3D representation and coordinate system of the incident scene and known, visible straight lines in the images, respectively. In some cases, such as investigations being done in rural or wooded areas with limited resources, these conditions may not be met. Also, manual correction may provide a cost-effective and fast method of generating corrected images when mainly concerned with visual presentation instead of performing accurate measurements. Overall, as there are some potential use cases for manual lens distortion correction, investigating the relative accuracy of said method compared to the control point and straight-line methods is beneficial.

2. Methodology

To assess the ability of several lens correction techniques to generate a corrected image, images with varying amounts of distortion were generated using Adobe Photoshop, 5 with barrel distortion and 5 with pincushion distortion. Control point, straight line, and manual lens correction techniques were then applied to these distorted images and the result compared to the initial, undistorted images. Locations of pixels were then compared between the corrected and idealized undistorted images to quantify the amount of unresolved error in the correction.

2.1. Generation of an idealized image

An idealized grid was created in Blender software version 4.3.2 (Blender, Amsterdam, Netherlands) because of its ease of use and integration of ideal virtual cameras. Two parallel grid planes were first defined and offset from one another, with one plane behind the other, to create a 3D object. For each plane, a grid was created, with the farther plane having a grid with larger distances between intersections, resulting in a 2-grid object. The virtual camera was then placed so that its optical axis was orthogonal to the planes, and an image was taken with a resolution of 1920x1080p. Due to the use of ideal virtual cameras, no distortion of the image occurred, and the image can be said to represent the true geometry of the grids.

2.2. Generation of distorted images

A set of 10 distorted images of the initial idealized grid (Fig. 1) were created for this study, 5 with barrel distortion and 5 with pincushion distortion (Fig. 2). These images were created using Adobe Photoshop's (V 26.4.1, Adobe Inc.) lens distortion plug in [40]. The images were distorted manually using this tool with scalar values of 10, 20, 30, 40, and 50 for both pincushion (P10, P20, P30, P40, P50) and barrel (B10, B20, B30, B40, B50) distortion. The degrees of distortion represent a scaled severity, rather than an absolute value, when using the lens distortion tool in Adobe Photoshop. Therefore, P10 is the least distorted pincushion image, while P50 is the most severely distorted. Adobe Photoshop follows a Brown-Conrady model for lens distortion correction [41], and therefore when applying distortions to generate or correct for

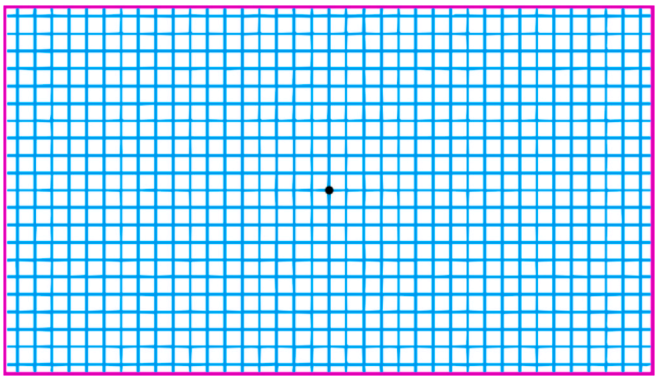

Fig. 1. Image of the idealized grid used to illustrate results. Note the colored border around the image is solely a visual addition to increase image clarity and was in no way utilized in any methodology steps indicated.

radial distortions in the manner specified above, allowing for easily accessible, reproducible levels of distortion.

2.3. Lens correction techniques

Each distorted image was corrected using control point, straight line, and manual correction methods. After correction, the difference in position of the pixels of interest was calculated to quantify how accurately the correction technique reconstructed the geometry of the images. This methodology was completed 5 times per technique per degree of distortion, resulting in 150 images total and 1500 data points (pixel shift distances).

2.4. Control point lens correction

For control point lens correction, a geometrically true 3D reference of the space or object seen in the image being corrected is required. To perform the control point correction, the 3D object file (a.STL), generated from the grids created and captured in the original, idealized image, was uploaded to PhotoModeler Premium software, version 2025.0.0.332 (PhotoModeler Technologies, Vancouver, British Columbia, Canada) alongside the distorted images. Points were placed on both the image and 3D object in locations which were clearly visible on both representations. A minimum of 25 common control points spread throughout the image are used for this technique to have optimal effectiveness when correcting for distortion through PhotoModeler's bundle adjustment algorithm [42]. Bundle adjustment is an iterative process used to solve for both the camera's location and orientation as well the distortion parameters simultaneously [12,43]. Due to the many variables to be solved during the process, the larger number of defined points aids in optimization. PhotoModeler does allow the user to override this minimum, however they recommend 25 points to provide a robust, optimized solution with a large amount of photo coverage, especially in areas of higher distortion, such as the edges of the image [42].The image and 3D reference were then overlaid so that the control points have the lowest culminative error point to point (i.e. each control point is a pair between the 3D model and image, the error is calculated for each of their pairs and then converted to an overall error representing the fit). Once complete, the image was undistorted in such a way that the error between the 2D and 3D control points was optimized by adjusting camera intrinsic and extrinsic parameters, as well as related distortion coefficients. The result of this warping was a lens corrected 2D image (Fig. 3) which was then exported for further use and analysis.

2.5. Straight line lens correction

Straight line lens correction was performed using PFTrack software (V 24.03.13, The Pixel Farm Ltd.). The distorted images were uploaded to the software, and the straight-line correction tool was chosen. At least three lines in the 2D image which are geometrically straight in the idealized image but appear curved in the distorted images were identified. Straight lines were drawn connecting 2 visible points along the identified curved lines. These drawn lines were then edited to follow the visible curve of the lines in the distorted image, maintaining the position of the 2 initial endpoints. Preference was given for lines further from the centre, to attempt to reach the optimal correction through lines placed in the most distorted regions of the image, though lines were often also spread throughout the image and centre. Line placements varied between sets and images. Once this was completed for at least 3 lines, to provide image coverage and provide information on the vertical, horizontal, and angled axes. the image was warped to find the solution in which all drawn lines were as straight as possible, resulting in the corrected image for lens distortion (Fig. 4).

2.6. Manual lens correction

Manual lens correction was completed using Adobe Photoshop's lens distortion plug in. The distorted images were uploaded to the software and manually corrected using the distortion slider provided. This slider is for a simplistic correction of images by defining the degree of pincushion or barrel distortion applied. Due to its manual nature, no optimization algorithm is present, and instead, the researcher judged when the 'optimal' correction was reached (Fig. 5). This was accomplished by oscillating the slider from low to high values repeatedly. Initially during correction, distortion would decrease. However, once the optimal correction was surpassed, visual distortion would begin increasing once more. The correction value would then be decreased, decreasing visual distortion. As the correction value decreased, it would at some point pass the optimal level and begin increasing visual distortion once more. This process would be repeated, providing an increasingly small band of correction values until the optimal correction level was determined. The visual distortion was made apparent by the remaining waves within the lines of the grid structure, seen within Fig. 5B. A wave with smaller deviation between the peaks and troughs was considered more corrected.

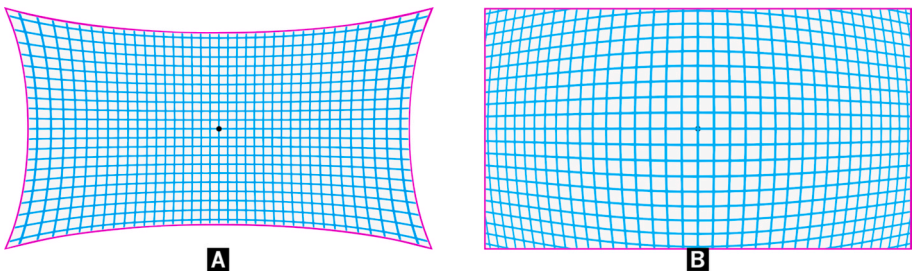

Fig. 2. (A) P30 pincushion distorted image. (B) B30 barrel distortion image.

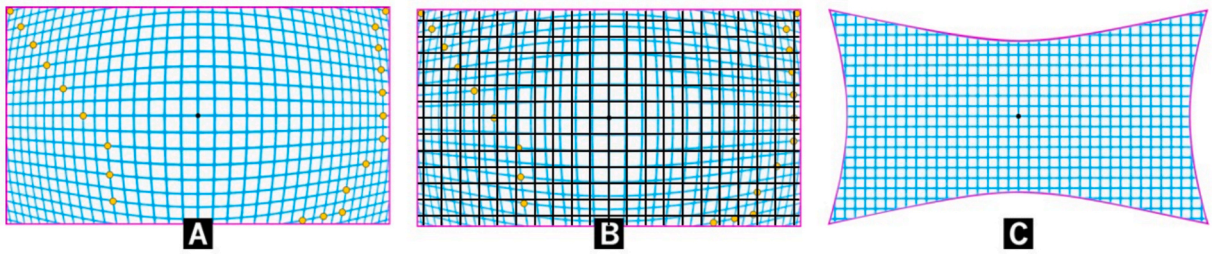

Fig. 3. An example of distorted and corrected images using control point lens correction technique. (A) The initial B40 distorted image. (B) B40 distorted image with an overlay of the 3D object STL file (black grid). The indicated yellow points seen in (A) and (B) are related to the same points on this 3D object and used to implement PhotoModeler's bundle adjustment algorithm. (C) The corrected image. (For interpretation of the references to colour in this figure legend, the reader is referred to the web version of this article.)

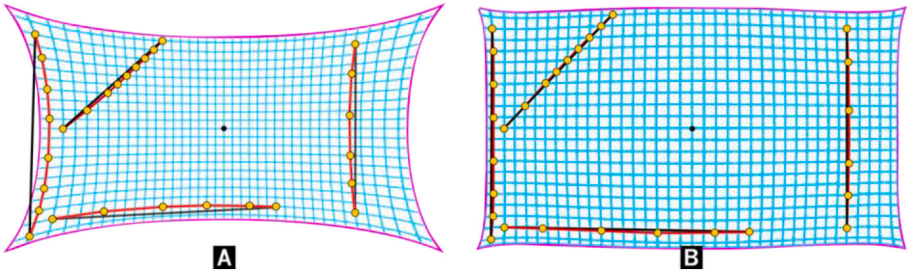

Fig. 4. An example of distorted and corrected images using straight line lens correction. (A) Distorted image with lines drawn to followed visually distorted curves. (B) Corrected image with lines showing degree of correction.

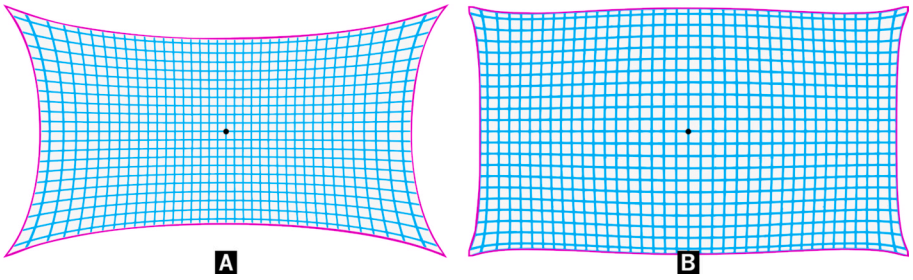

Fig. 5. An example of distorted and corrected images using manual lens correction. (A) Distorted image. (B) Corrected image.

2.7. Measurement of pixel errors

Prior to performing measurements, the resultant corrected images were aligned with the idealized initial undistorted image. Firstly, if the correction technique led to a change in frame size, the images were resized to the original 1920x1080p size following correction using Adobe Photoshop's bicubic smoother algorithm, based on bicubic interpolation [44]. The images were then further aligned by forcing the respective image centers and corner measured points to overlap. This was done to remove the effect of scale and translation resulting from the corrections, and to isolate only the accuracy of the correction itself when determining pixel movement errors. In some instances, if the correction resulted in removed sections of the image (often removal of the corners), pixel error measurement could not be completed as the above alignment procedure could not be applied correctly. Error in correction accuracy was defined through the position of pixels spread throughout the images. On the idealized image, pixels at the centre of gridline intersections were used as points of comparison for all corrected images. 11 of these pixels were chosen for analysis, located along the diagonal from the centre of the image to the top right corner to capture the full radial distance from the centre, placed at equidistant line intersections to provide simple re-picking for measurements. This also included the image centre. The first point, other than the image centre, was vertically offset from the centre of the image to allow for equidistant spacing while covering the full radial distance of the image. The location of these

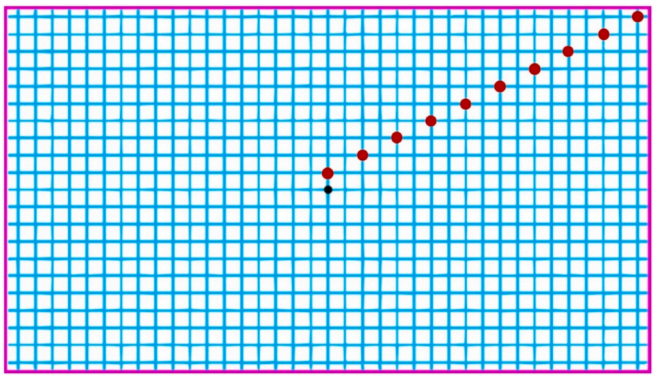

Fig. 6. The idealized grid image, also seen in Fig. 1. The marks seen represent the points chosen for the 11 pixel movement measurements, with the black mark being placed at the image centre. These red markers are for visual clarification only. The underlying grid intersections were used as references for the measured points. (For interpretation of the references to colour in this figure legend, the reader is referred to the web version of this article.)

points can be seen in Fig. 6. These same pixels were also located in all corrected images and the change in position between the idealized and corrected images was measured. This change was defined by a distance value determined by first measuring the initial true X and Y coordinates of the pixels of interest. The same was done for the corrected images. These two coordinates were then compared to calculate the amount of shift remaining in the corrected image compared to the idealized image at the 11 indicated points.

2.8. Quantification of manual pixel picking error

In order to quantify the error associated with the manual method of selecting pixels, a re-picking error was defined. This test was completed by the researcher who also conducted the pixel movement measurements and therefore cannot be generalized. First, a known pixel location at a single determined line intersection in the image displayed in Fig. 1 was defined. Then, this pixel was manually chosen 20 times and the location of each measurement recorded. The mean and standard deviation of the error between the known and manually measured pixel location was calculated as an absolute distance. The error between the measured and known positions was first measured in its X and Y components and the radial distance calculated. The reported mean and standard deviations were calculated over these radial distances. This measurement can be used to then quantify the human error associated with the choice of measured pixel to give insight into the attribution of the measurement process to the recorded errors from the correction techniques described above.

2.9. Qualitative assessment of correction techniques on a Real-World image

As the methodology used throughout this paper focuses on an ideal digital image with digitally generated distortions, it does not account for other factors found in real-world applications of forensic photogrammetry. This may include lighting, noise, exposure, and other such factors present in physical photography [45,46].

Therefore, a simulated incident scene was photographed and the above correction techniques, control point, straight-line, and manual correction, were applied to the images. One photograph was taken with a GoPro Hero 8, set to wide angle view with a standard lens at 1.4x zoom, resulting in an image with a resolution of 2700x1520 pixels. This camera was chosen as it presents a noticeable level of visual distortion without being extreme, while providing a good field of view to capture the entire scene at a reasonable distance. The second image was taken with an Axon Body 2 camera, a body worn camera intended for use by law enforcement, with a resolution of 848x480 pixels. This image was used as the level of distortion present is higher than with the GoPro camera. The images are taken from different perspectives and locations in the scene, with the AXON Body 2 positioned closer to the scene due to its lower resolution, in order to ensure sufficient image clarity and sharpness of features required for each of the 3 correction techniques.

In Fig. 7, the 2 images can be seen. Fig. 7A, the image taken with the GoPro camera, is representative of a low severity barrel type distortion when compared to Fig. 2A, B30 (medium) level distortion. Note the curved lines along the fence on the left side of the image, on the building edges along the right side, and in the garage covering near the top of the image. In Fig. 7B, it can be clearly seen that is shows a higher level of distortion than 6A, most clearly demonstrated by the curvature of the upright steel supports. Both images display a barrel type distortion.

To facilitate reasonable use of all 3 correction techniques, the scene also includes straight lines, in the form of edges of buildings, rooftops, fencing, and pavement lines, which can be expected to be sufficiently straight and common in real-world applications. In this use case, all features used as straight references in Fig. 7, and all subsequent related Figs. 11-13 have been confirmed to be straight on site. For the purpose of control point correction, a 3D scan of the scene was also taken using a Dot3D DPI-10-SG structured light scanner with an Intel RealSense D415 stereoscopic depth sensor attachment. The maximum scanning range (from sensor to surface) was kept below 1.5 m based on the recommendation of the manufacturer and published works [47,48]. This can be expected to maintain a depth error in the resulting scan of approximately 0.509 ± 3.9 mm [48]. Additional scan control points in the form of patterned physical markers, also known as April Tags, were also included to aid in minimizing scan drift over the volume of the scene.

After distortion correction using the 3 techniques being analyzed in this study, the photographs were compared qualitatively for any noticeable difference in the level of correction between the 3 methods.

3. Results

3.1. Idealized digital Images: Pixel position error

Fig. 8 displays the pixel position error in the corrected images relative to the true position in the initial idealized grid averaged over all distortion conditions per radial distance. As can be seen, the straight-line and manual methods show much larger errors and standard deviations for the barrel distortion type than the pincushion distortion. When comparing the manual and straight-line techniques, it can be seen that their correction errors are comparable. However, the straight-line technique does seem to have lower pixel accuracy results than the manual technique at higher levels of barrel distortion. The control point technique demonstrates a high level of consistency in both error and standard deviation across all radial distances and distortion types.

3.2. Idealized digital Images: Pixel position error relative to distortion type and severity

In Figs. 9 and 10, pincushion and barrel distortion results are displayed separately. Each figure shows the distortion correction error in pixel position for each severity and technique. The values displayed represent the average corrected pixel position error, when compared to the known true position, over all 5 sets for each distortion type, severity, and correction technique.

As seen in Figs. 9 and 10, for higher levels of distortion of 30, 40, and

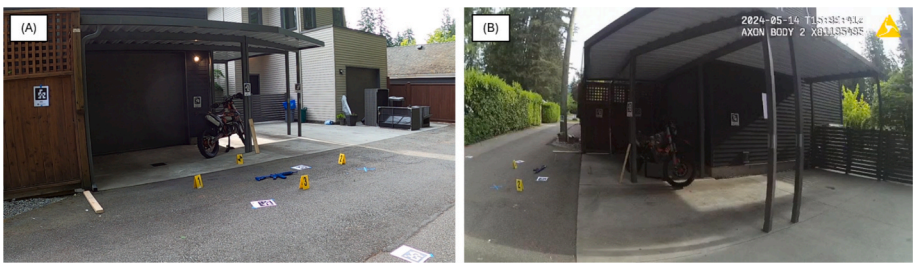

Fig. 7. The photographs used in the qualitative assessment of real-world application of the 3 distortion correction techniques. (A) The image taken by the GoPro Hero 8. (B) The image taken by the Axon Body 2.

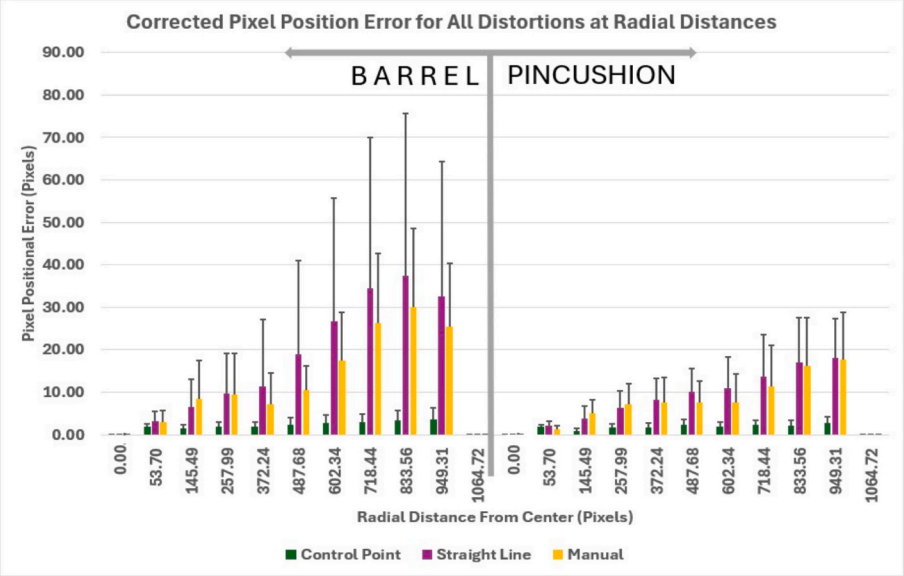

Fig. 8. Mean pixel position errors following correction with each of the 3 techniques. Means are calculated over every distortion severity but are separated based upon distortion type. Error is defined as the difference between the corrected pixel position and the known pixel position measured in the ideal image pre-distortion (ideal image is displayed in Fig. 1). Error bars show standard deviation of the mean errors. Test image size is 1920 x 1080p.

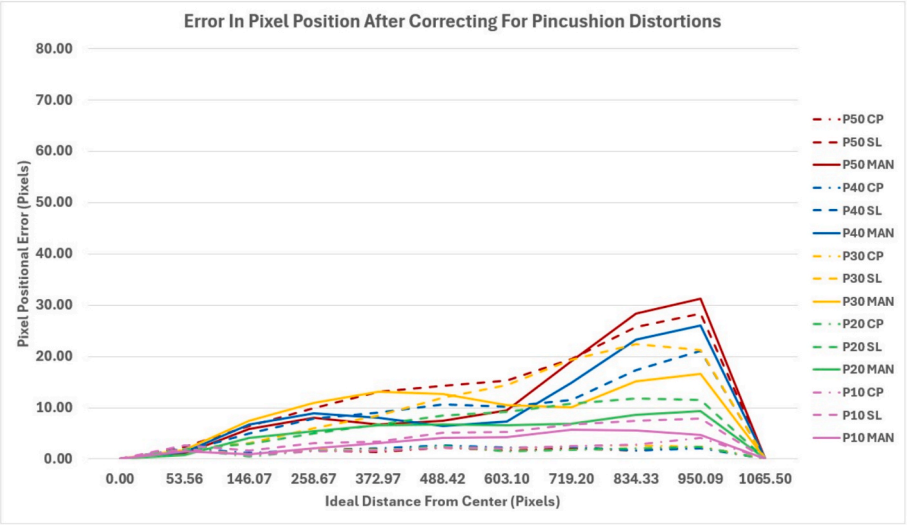

Fig. 9. Error in corrected pixel position following distortion correction using control point, straight line, and manual correction on pincushion distorted images. Errors have been averaged over all 5 data sets, in which each line / category represents a set of 5 measurements specific to each distortion correction type and distortion severity. Error is calculated as in Fig. 8.

50, the highest error does not occur at the farthest distance from the centre, but rather around 834.33, for the barrel distortions, to 950.09 pixels, for the pincushion distortions, from the centre, or approximately 77% to 88% of the radial distance. For barrel distortion, manual and straight-line correction are initially similar in their error measurements, however the straight-line technique quickly has higher errors than the manual technique at a distortion level of B30 and above. For the pincushion distortion type, the two techniques do not produce as severe of a gap in error measurements, with all resultant errors much more clustered than as in the barrel distortion. Compared across the 2 distortion types, straight-line correction presents the biggest accuracy difference, performing far better for pincushion distortion. Moreover, the control point technique has a consistently lower error across both distortion types and distortion severities, maintaining an average error of well below 10 pixels at every radial distance. A further breakdown of Figs. 9 and 10 can be found in Appendix A.

3.3. *Idealized digital Images: Manual pixel picking error*

The manual pixel picking error, determined by the mean and standard deviation of 20 measured pixel locations relative to a known pixel location, is 0.22 ± 0.12 pixels. This represents approximately 41% of the lowest measured corrected pixel position error using the digital images and the 3 correction techniques, which was 0.53 pixels for the P20 manual technique at a radial distance of 146.07 pixels from the centre of the image. Relative to the largest error of 79.40 pixels, resulting from straight-line correction of the B40 distorted image, this pixel picking error represents approximately 0.3% of the correction error.

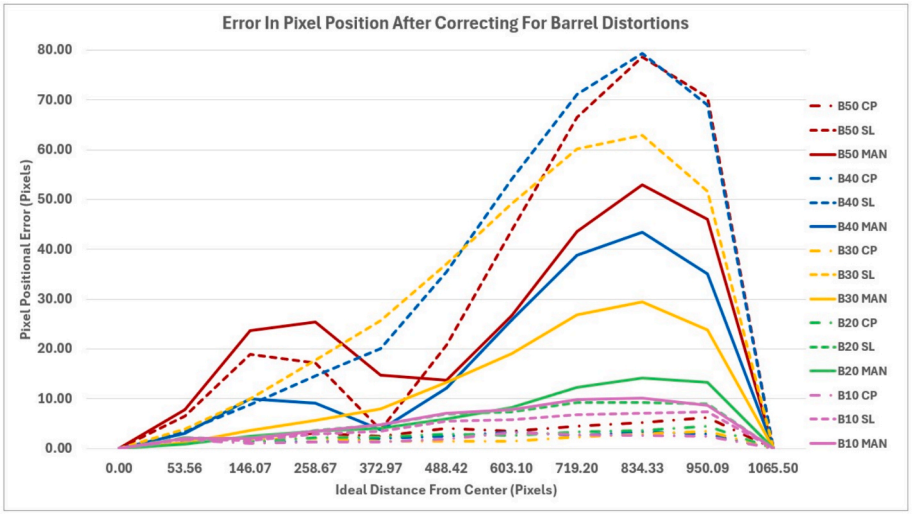

Fig. 10. Error in corrected pixel position following distortion correction using control point, straight line, and manual correction on barrel distorted images. Errors have been averaged over all 5 data sets, in which each line / category represents a set of 5 measurements specific to each distortion correction type and distortion severity. Error is calculated as in Fig. 8.

3.4. Qualitative assessment of correction techniques on a Real-World image

Figs. 11 and 12 below display the results of applying control point, straight line, and manual correction to real-world images. Fig. 11′s original, uncorrected image is shown in Fig. 7A as captured using the GoPro Hero 8, and Fig. 12′s uncorrected image in Fig. 7B as captured using the Axon Body 2. Fig. 11 shows that the applied correction resulted in mostly similar images, with no obvious differences to the straightness of object references seen when closely viewing objects of reference, such as the vertical steel supports. For Fig. 12, the resulting corrected images vary to a higher degree, both in the resulting shape of the image, and the level of remaining distortion.

4. Discussion

Based upon the results of this study, control point lens correction clearly appears to be the most accurate correction method, as shown in the results of Figs. 8-10, maintaining a pixel correction error of well below 10 pixels. While the control point lens correction method consistently presents the lowest error and deviation across distortion type and severity, as shown in Fig. 8, it can also be seen in Figs. 9 and 10 that the comparative relationship between the straight-line and manual methods differs for pincushion and barrel distortions. In the pincushion distortion, the two techniques remain much closer in terms of their associated pixel correction error. However, in barrel distortion, at a distortion level of B30 and above, the straight-line technique shows much higher errors than the manual. For example, in B40, the straight-line error ranged from a 3.45 pixel error near the centre of the image, to a maximum of 79.40 pixels. For the manual technique, errors ranged from 3.05 pixels near the centre to 43.39 pixels at the maximum. As such, it could be said that the manual method was more accurate for higher distortion image correction relative to the straight-line method, while they were more comparable at lower distortion levels. This is further reinforced when examining Fig. 8. It can be seen that for barrel distortion averaged over all levels of distortion, straight-line correction

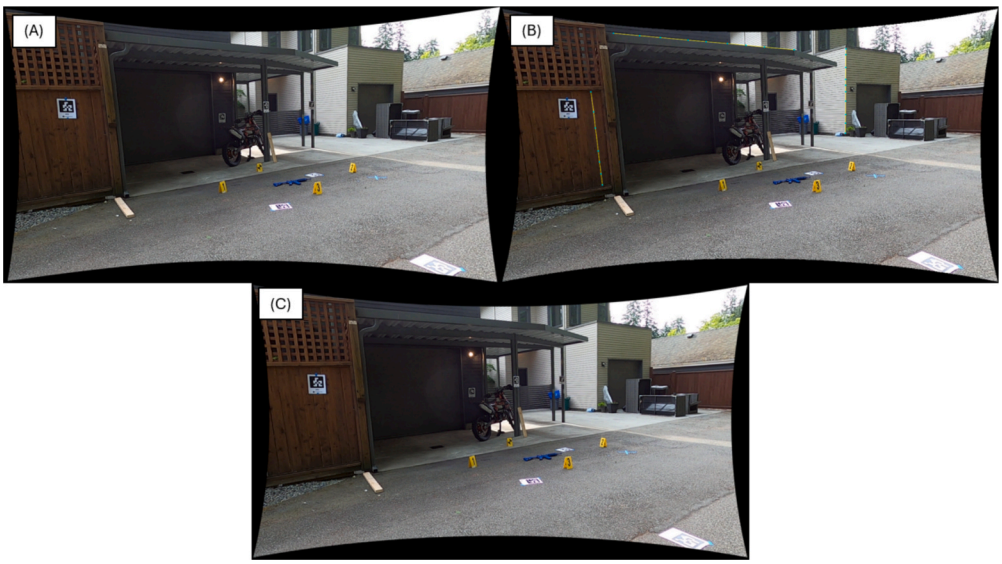

Fig. 11. Images captured by a GoPro Hero 8 camera, corrected using the studied techniques. (A) Corrected using control point lens correction. (B) Corrected using straight-line lens correction. Lines used presented as yellow lines with blue segment markers. (C) Corrected using manual lens correction. (For interpretation of the references to colour in this figure legend, the reader is referred to the web version of this article.)

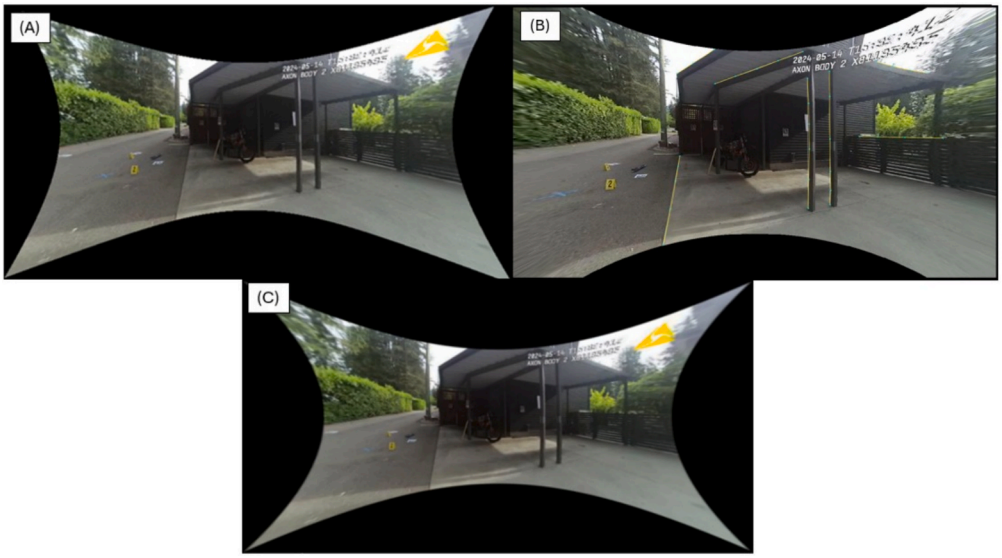

Fig. 12. Images captured by an Axon Body 2 camera, corrected using the studied techniques. (A) Corrected using control point lens correction. (B) Corrected using straight-line lens correction. Lines used presented as yellow lines with blue segment markers. (C) Corrected using manual lens correction. (For interpretation of the references to colour in this figure legend, the reader is referred to the web version of this article.)

has clearly higher errors and standard deviations associated with it. However, for the pincushion distortions displayed in Fig. 8, the values of the manual and straight-line methods remain comparable. Regardless, this demonstrates that the manual and straight-line methods both perform better for pincushion distortion than barrel distortion, especially at higher distortion severities.

Although the control point method consistently outperformed the others, we must also take into account the effect of the lens correction models used by the software as well as the technique themselves. PhotoModeler's control point correction has the ability to define K1, K2, K3, P1, and P2, which are used in equations (1) and (2) along with the parameters characterized in Table 1 to define distortion correction [42].

$$dr = K1{*}r^2 + K2{*}r^4 + K3{*}r^6 \tag{1}$$

$$dpx = P1{*}\left(r^2 + 2{*}x^2\right) + 2{*}P2{*}X{*}Y \tag{2a}$$

$$dpy = P2{*}\left(r^2 + 2{*}y^2\right) + 2{*}P1{*}X{*}Y \tag{2b}$$

This allows for a wide range of distortions to be properly corrected. However, for the straight-line and manual techniques, the correction model seems to be more limited, likely using a simplified version of the above model equation or another simplified model, possibly also explaining the remaining wavy lines post-correction seen in the straight-line and manual corrected images at higher distortions. This remaining distortion can be seen in Figs. 4B and 5B clearly.

Table 1
Distortion correction parameters used by PhotoModeler.

Variable	Definition
dr	Radial change of pixel point from radial distortion correction and can be further broken down to x and y components
r	Radial distance from principal point
***K*1**	2nd order polynomial radial distortion coefficient
***K*2**	4th order polynomial radial distortion coefficient
***K*3**	6th order polynomial radial distortion coefficient
dpx	Change in X position of pixel point due to decentering distortion correction
dpy	Change in Y position of pixel point due to decentering distortion correction
***P*1**	Decentering distortion correction coefficient
***P*2**	Decentering distortion correction coefficient
X	X position of pixel point from principal point
Y	Y position of pixel point from principal point

Moreover, as this study relied on manual selection of corrected pixels for measurement, the error associated with the human selection was quantified to determine if it would have any significant effect on the results and conclusions drawn from them. It was found that, over 20 trails of selecting a pre-determined, known pixel, that the average resulting error in pixel position was 0.22 ± 0.12 pixels. While likely not significant to the overall trends and findings of the study or in cases with already large errors, this number represents a relatively large error compared to the more accurate corrections. Therefore, it must be considered when further interpreting values such as those for control point correction and low distortion severity corrections. Additionally, some images had to be resized to the original dimensions to perform accurate measurements. The use of a bicubic interpolation algorithm for this process may introduce additional noise and error into the resized image, affecting resultant measurements.

Literature on the topic of image distortion correction for forensic applications focuses mainly on the downstream effects on physical measurements made through photogrammetric techniques using the image. Thus, these studies' results are the product of the entire pipeline of steps required for these measurements, including the measurement technique itself, distance from the camera to the subject, and the experimental and photography conditions used. This makes their conclusions somewhat specific to the context of the study other than any supported overall trends. However, the present study eliminates the downstream measurements and isolates the image distortion correction process based on measurement of corrected image pixel error rather than any physical measurement, which would be dependent on the experimental conditions and setup and therefore not necessarily generalizable to all applications. Thus, the experimental procedure and use of pixel measurement on digital images is done with the intention to inform forensic investigators on which correction technique is best suited for their application regardless of further measurements to be made.

For example, a study conducted by Terpstra et al. in 2017 [19], involved a test with a simulated road incident scene. Markers were placed within the scene to represent relevant evidence and photographed with 3 physical cameras. The scene and marker locations were first recorded using a 3D scanner and total station. The images taken by the on-site physical cameras were then lens corrected using both control point and straight-line correction, similar to as described in the present

study. Following lens correction, the images were then used for photogrammetry to locate the 3D position of the markers through the 2D images. The measured marker locations were then compared to the known location from the previously completed scene documentation. The result was that the control point correction technique resulted in a position error of 11.3 cm on average while the straight-line correction technique led to a position error average of 9.9 cm [19]. This implies that the straight-line lens correction technique leads to slightly better or comparable results when used as an initial step in determining the location of missing evidence or relevant features of an incident scene. This is contrary to our results which showed clear superiority of the control point technique over the straight-line method. While not a direct comparison as the present study looked solely at the lens distortion correction accuracy and not the downstream effect on photogrammetric measurement accuracy, the superiority of the control point technique as found in the present study would be assumed to also carry over at least partially into photogrammetric measurements. This inconsistency may be due in part to the specific conditions, images, use of physical cameras, levels of distortion, and techniques in terms of line placement or image control points, creating an environment more suited to straight-line correction over control point correction, though this is difficult to say concretely. The study also does not specify the number of common control points used, making it difficult to compare to our methodology. It must also be noted that both Terpstra et al. and this study used the same software, and therefore the same correction algorithm, for the straight-line technique, but different software for the control point method. Lastly, further analysis of the data presented in Appendix B of the study by Terpstra et al. shows that the control point method did actually outperform the straight-line method in some cases depending on the camera being used and its location. As seen in Appendix A of Terpstra et al.'s study, the images used represent low distortion severity, likely approximately equal to B10 or B20, in which case it is expected, as per the results of the current study, for the corrections to perform more similarly than for higher distortion conditions [19].

Another study, by Tosti et al, in 2021 [6], compared the measured height of a subject in images corrected for lens distortion using a ground control point calibration method, where the control points are determined through a Terrestrial Laser Scanner, and the straight-line method, in Amped FIVE Software. The images used here were much more heavily distorted than for the study by Terpstra et al. discussed above. Following lens correction, the same method was used to measure subject height regardless of the correction method used prior. Subject height was determined by defining a plane parallel to the floor of the scene and then defining a point at the intersection of two lines connecting the heel of one foot to the toe of the other. The height measurement is then determined by an offset from the ground plane above the defined point. The authors note some subjectivity with this method, and therefore performed repeated measurements in cases where sections of the feet where occluded. The results of the study demonstrated that the ground control point method was more accurate than the straight-line method when measuring subject height, with mean errors over 4 subjects ranging from 0.1 to 3.4 cm and 1 to 7.6 cm, respectively [6]. This result, when combined with the information from Terpstra et al, 2017 [19], appears more consistent with the results of the present study. With the less heavily distorted images found in Terpstra et al [19], the control point and straight-line correction techniques perform more similarly. Whereas with more heavily distorted images, the control point technique outperforms the straight-line method, as in Tosti et al [6]. This same relationship can be seen in Figs. 9 and 10, in which the 3 techniques start off more closely in respective error, but as the distortion level increases, the error in the straight-line technique becomes larger relative to the control point method.

While this study focuses mainly on the application of the correction techniques to a digitally generated image, the application of them on real-world cases introduces many variables not accounted for in this study. This possibly makes these results not as generalizable to all conditions, as was demonstrated by the discussion of Terpstra et al, 2017. These include other camera-based factors, such as resolution, frame rate and exposure, scene-based factors such as lighting, and other factors such as file compression during transmission [45,46]. As such, a limited proof of concept test was conducted using real-world images, seen in Fig. 7, corrected for lens distortion using the 3 methods. The results, shown in Figs. 11-13, demonstrate correction capabilities consistent with those found using the idealized test grid digital image.

For the low distortion severity image found in Fig. 7A, no visual difference of any significance could be seen between the 3 correction techniques. For the low severity, B10 and B20, results seen in Fig. 10, the 3 correction techniques result in relatively low pixel position errors, though the control point method does still see lower errors than the others. For the higher distortion severity image shown in Fig. 7B, the resulting correction difference is more noticeable between the three lens correction methods.

In Fig. 12, the corrected images from the Axon Body 2 camera, the control point technique appears to have given the best correction, but only a visually slight improvement over the straight-line method. The manual method appears to have generated the least accurate correction. It can also be seen that the straight-line method resulted in a less 'zoomed out' corrected image that the other techniques. In Fig. 13, a

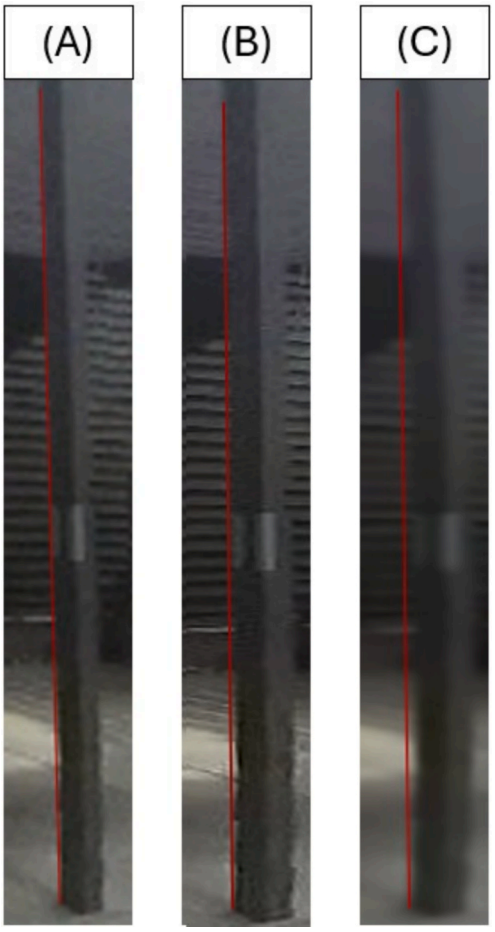

Fig. 13. A vertical steel beam used as a qualitative measure of the level of correction of the image captured by the Axon Body 2 camera, displayed in Fig. 7B in its original, distorted form, and in Fig. 12 in the resulting corrected forms. (A) Corrected using control point correction. (B) Corrected using the straight-line technique. The line used for the correction is removed for uniformity of comparison to the other images. (C) Corrected manually. Note in (B) and (C) the visible building siding and ground appearing between the red line and beam edge. (For interpretation of the references to colour in this figure legend, the reader is referred to the web version of this article.)

close-cropped subsection of the corrected images from Fig. 12, the vertical support beam in Fig. 13A appears to be mostly straight. In Fig. 13B, the straight-line correction result, it appears to have generated a correction result somewhere between the manual and control point methodologies, with a slight visual curve remaining in the beam, noticeable as the slight gap between the line and beam in sections. Moreover, it can be seen that in Fig. 13C, the manual technique resulted in a blurrier image relative to the other methods, likely due to 'stretching' of the image required in the correction.

Though only a limited qualitative analysis, this test demonstrated that the control point technique functions well under real-world conditions, while the straight-line method performs as a close second and the manual method could not fully correct the image with higher distortion. However, it is important to note that in some cases, photography may be necessary to occur in a dark environment, such as for time-sensitive incident scene photos occurring during the night. When using all techniques, lighting and contrast between background structures impeded correction. For the control point technique, some sections of the image, such as on the walls under the overhead covering near the motorcycle, were too dark to reliably pick control points. For the straight line and manual techniques, the lack of contrast between the vertical steel beams and the background, made them difficult to use as accurate references for either the placement of a reference line or visually. The uncorrected image with the lines to be used in the straight-line technique can be seen in Fig. 14. Therefore, as per forensic photography guidelines, care should be taken to properly illuminate the scene prior to imaging [16–18]. In all cases, the resolution of the cameras made accurate selection or reference difficult when considering features which were physically farther away from the cameras.

This study was conducted to aid in informing forensic investigators about their options when it comes to lens correction of photos to be used for further measurement and analysis. As discussed above, the digital nature of the setup does not include many confounding factors present in physical photography. As such, it is also important to note how these results can be applied to real-world investigations. Firstly, this study focused on radial distortions and did not include non-uniform, tangential or other sources of distortion in the main digital image correction section of the paper. However, it is noted that radial distortion is the most significant factor in image distortion and tangential only plays a small part, though this should be investigated further in the future [6]. Given that this study measured pixel error instead of any physical measurement made in centimetres or millimetres, it is difficult to understand how these orders of error may affect measurements made. Errors in pixel position will propagate into physical measurements made using the 2D images dependent on distance, as a single pixel will cover a larger physical space at a distance of 10 m from the camera than at 1 m. Therefore, investigators must be aware that distance to the object or persons of interest, among other factors, not only affects the visible resolution of the image relative to the subject, but also the resultant measurement error. The control point correction technique's maximum 6.24 pixel error may result in an error of 1 cm at shorter distances or in good conditions, and an error of 1 m in poor conditions at farther distances. When applied to forensics, this distance-dependence could result in mis-measured subject height, impact velocity, or other important measurements. Thus, the effect of the pixel error on actual measurements will need to be determined on a case-by-case basis by the investigator. Lastly, due to the relatively simple geometry of the 3D structure of the 2 offset planes creating discrete depths in which control points may occupy from the camera, it is possible that the results of this study may be somewhat more accurate than when to compared to more complex real-world sites.

Each correction method also has benefits and drawbacks which should always be taken into account. For the control point technique, the use of a 3D site scan and the additional positioning of the camera in 3D space relative to it, is a benefit for forensic investigators. However, like the other methods, it can suffer when images have poor lighting, heavy shadowing, or low resolution making it difficult to accurately select reference points. Therefore, an optimal application of this technique is in well lit, feature-rich environments with good lighting of all surfaces.

For the straight-line technique, it requires that known straight lines be present in sufficient length, quantity, and image coverage, making it more suited to urban environments than, for example, wooded or rural ones. Contrast is also a significant factor as it allows for clear distinction of straight lines from the background. Moreover, the straight-line method was more likely to cut off sections of the image during barrel distortion correction, especially at levels B40 and B50, as seen in Fig. 15. In some cases, it was possible to keep these corners present in the corrected image, but this generally resulted in these sections being 'stretched', generating artificially large errors in these areas as the

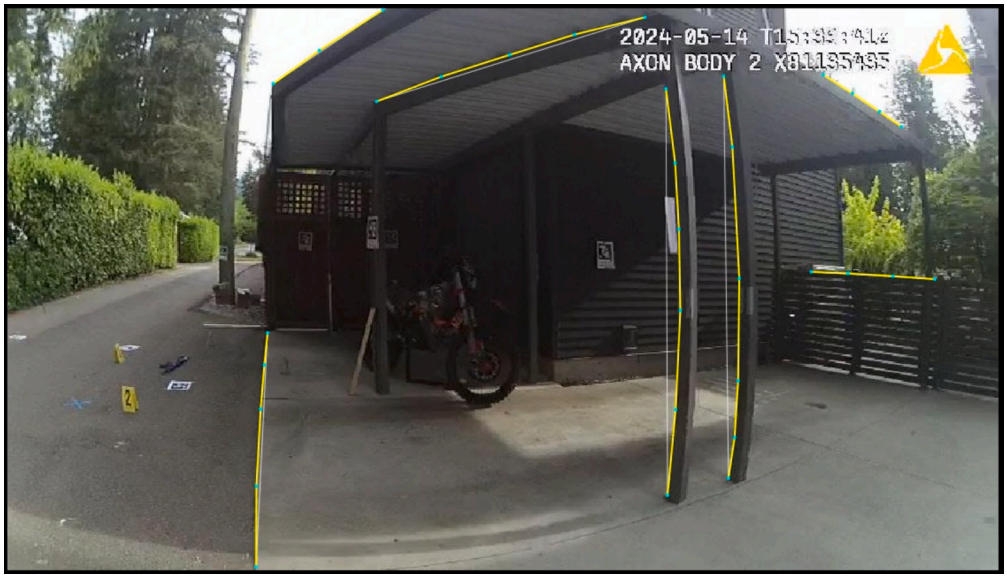

Fig. 14. The uncorrected image with the lines which would be used to perform the straight-line correction, of which the result can be seen in Figs. 12 and 13. Note the lack of contrast between the vertical beams and building wall, the shadowing effect near the garage door, and the low resolution of the fence on the right-middle side of the image.

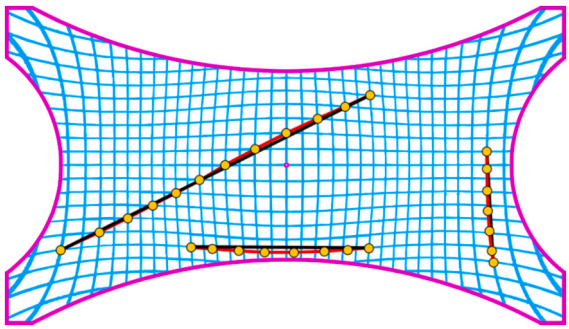

Fig. 15. An example of the edges of the image being cut off in straight-line correction for barrel distortion.

technique used had to be forcefully applied in a non-optimal way. This may cause an unacceptable loss of information in some forensic applications where objects or persons of interest are located near the edges of the image. However, it is important to note that not all software or correction algorithms will result in cut sections of the image, even using the same image and correction methodology.

The manual method, while displaying generally higher or comparable accuracy to the straight-line method depending on the distortion severity, suffers from subjectiveness. In forensic investigations with a legal implication, the expertise of the investigator using this method may be drawn into question. However, as long as sufficient visual reference is available to determine when correction is complete, it can be used in a wide variety of situations. An additional benefit, as with the straight-line technique, is that is does not require the use of a 3D site scan, which may not always be feasible for investigators to acquire. Lastly, as discussed with the real-world test image in Fig. 13C, the manual correction may negatively impact the visual quality of the image more than the others. As manual correction does include some level of subjective judgement on the side on the user, it is recommended that any further research into this methodology include both inter and intra-rater reliability measures.

5. Conclusions

This study aimed to add to the body of forensic photogrammetry literature by analyzing the accuracy of various correction techniques in isolation from specific physical experimental setups and measurements which may limit their generalizability. Based on the results of the present study, noting the small sample size and relatively simplistic distortion patterns, it is suggested that there is a hierarchy of techniques for correction of image distortion. Control point correction using a 3D scan should be the first choice when possible. Otherwise, the straight-line technique should be used, unless for some reason it is not feasible, in which case only then should manual correction be attempted. While it is reasonable to argue that the manual method produced smaller errors, and therefore should be used before the straight-line method, the subjective nature of the methodology suggests that it would be less reliable for forensic investigations and that the capability of the expert performing the correction could be called into question and would play a large role in the acceptability of the corrected image as evidence. Therefore, the manual correction technique cannot be recommended for forensic investigations when the other, more objective methods, are available. Regardless, given that the control point method outperforms the other two techniques and provides additional camera location information, steps should be taken to adopt this method for lens correction, when possible, though certain conditions may call for or necessitate use of the other methods.

CRediT authorship contribution statement

Kevin Gilmore: Writing – original draft, Software, Data curation. **Geoffrey T. Desmoulin:** Writing – review & editing, Supervision, Resources, Project administration, Funding acquisition, Conceptualization.

Declaration of competing interest

The authors declare that they have no known competing financial interests or personal relationships that could have appeared to influence the work reported in this paper.

Appendix

Appendix A:. Graphs showing corrected pixel position error relative to correction Method, distortion Type, and distortion severity

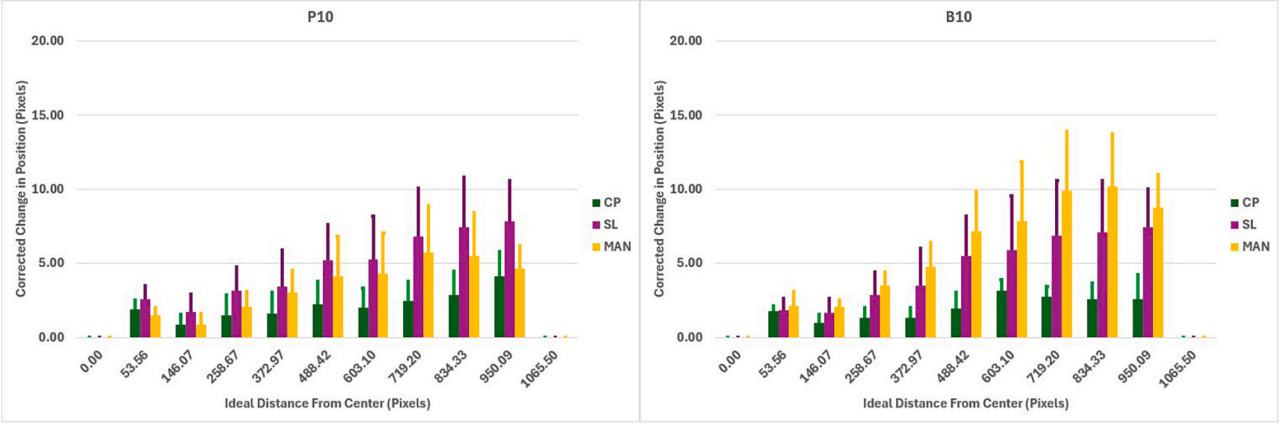

Fig. A1. P10 and B10 remaining distortions following lens correcting using the three techniques.

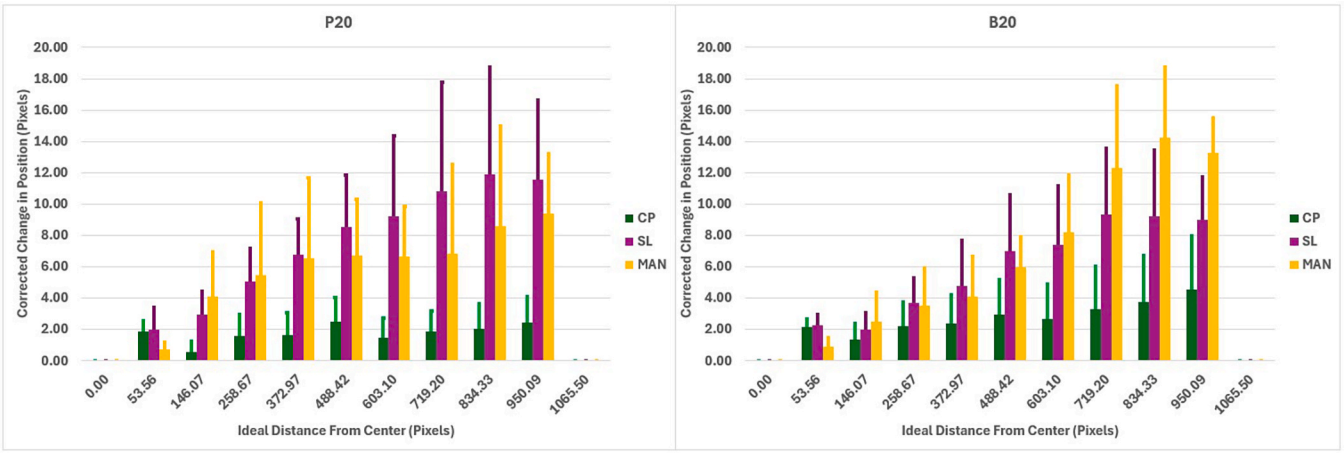

Fig. A2. P20 and B20 remaining distortions following lens correcting using the three techniques.

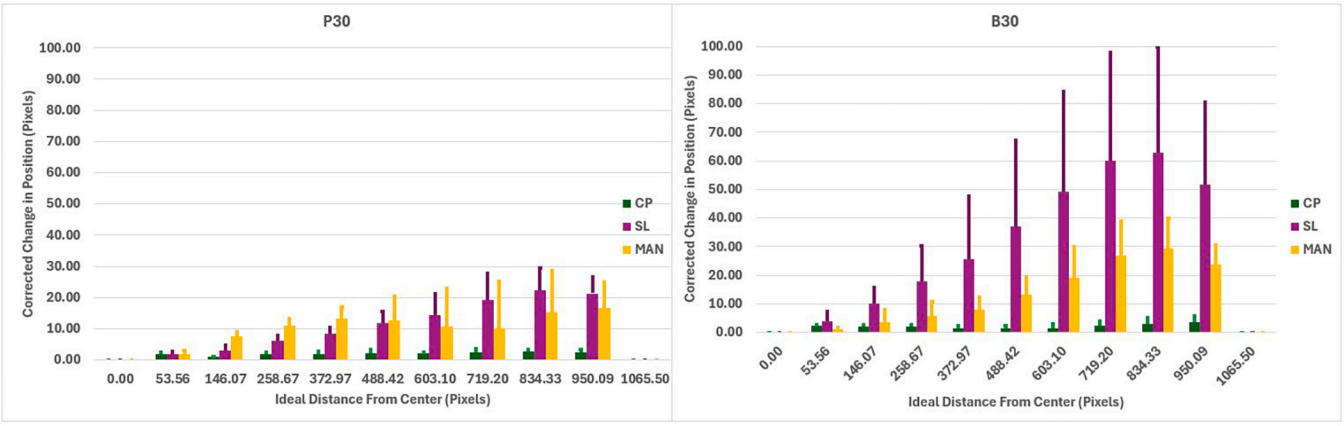

Fig. A3. P30 and B30 remaining distortions following lens correcting using the three techniques.

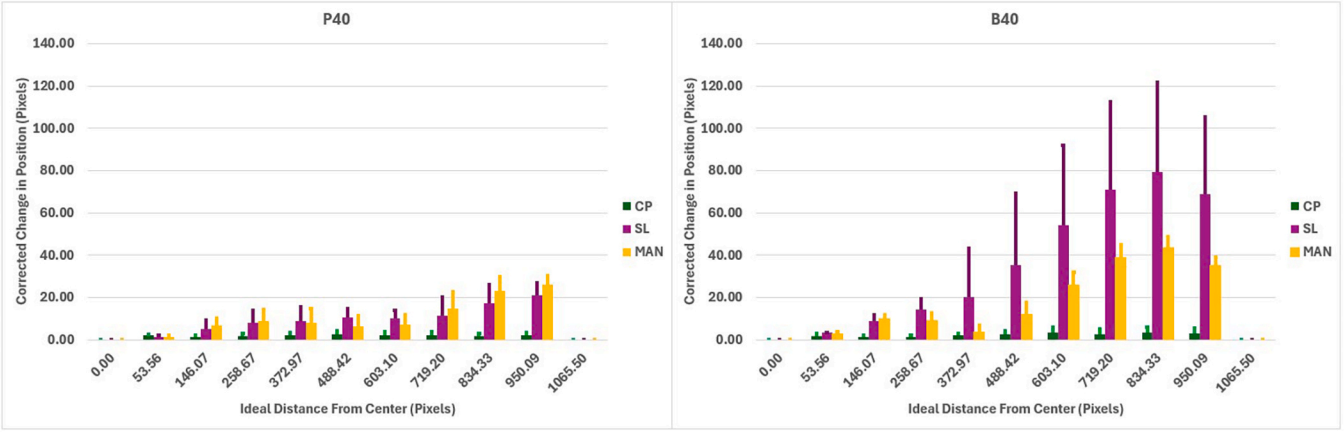

Fig. A4. P40 and B40 remaining distortions following lens correcting using the three techniques.

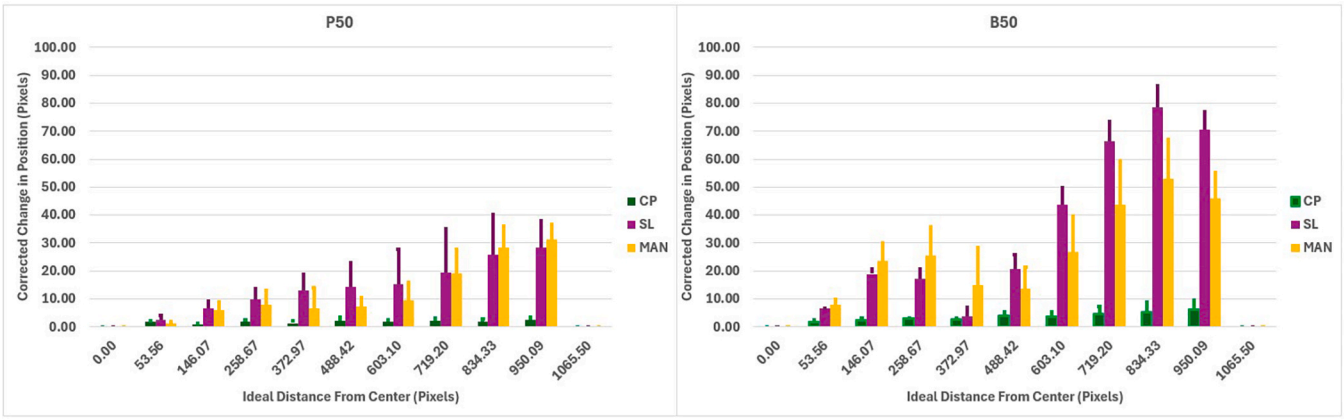

Fig. A5. P50 and B50 remaining distortions following lens correcting using the three techniques.

References

[1] B. Pan, L. Yu, D. Wu, L. Tang, Systematic errors in two-dimensional digital image correlation due to lens distortion, Opt. Lasers Eng. 51 (2013) 140–147.

[2] V. Chari, A. Veeraraghavan, lens distortion, radial distortion, in: K. Ikeuchi (Ed.), Computer Vision, Cham, Springer, 2021, pp. 739–741.

[3] W. Hugemann, in: Correcting Lens Distortions in Digital Photographs, European Association for Accident Research (EVU) Conference, 2010, p. 19.

[4] W.T. Neale, D. Hessel, T. Terpstra, Photogrammetric measurement error associated with lens distortion,, SAE Technical Paper (2011) 2011–01-0286.

[5] E. Liscio, H. Guryn, Q. Le, A. Olver, A comparison of reverse projection and Photomodeler for suspect height analysis, For. Sci. Int. 320 (2021) 110690.

[6] F. Tosti, et al., Human height estimation from highly distorted surveillance image, J. For. Sci. 67 (2021) 332–344.

[7] B. Hoogeboom, I. Alberink, Measurement uncertainty when estimating the velocity of an allegedly speeding vehicle from images, J. For. Sci. 55 (2010) 1347–1351.

[8] C.C. Chou, et al., Image analysis of rollover crash tests using photogrammetry, SAE Trans. 669–685 (2006).

[9] D.L. Gyemi, D.M. Andrews, R. Jadischke, Three-dimensional video analysis of helmet-to-ground impacts in north American youth football, J. Biomech. 125 (2021) 110587.

[10] M. Davoudkhani, C. Mulsow, H.-G. Maas, Single camera 6-DOF object tracking using spatial resection based techniques, Int. Arch. Photogramm. Remote Sens. Spatial Inf. Sci. (XLVIII-G-2025 (2025)) 351–358.

[11] T. Luhmann, Precision potential of photogrammetric 6DOF pose estimation with a single camera, ISPRS J. Photogramm. Remote Sens. 64 (2009) 275–284.

[12] T. Luhmann, W. Tecklenburg, 3-D object reconstruction from multiple-station panorama imagery, ISPRS Arch. 34 (2004) 5.

[13] T. Luhmann, Eccentricity in images of circular and spherical targets and its impact on spatial intersection, Photogramm. Rec. 29 (2014) 417–433.

[14] G.T. Desmoulin, M. Kalkat, T.E. Milner, Forensic application of inverse and reverse projection photogrammetry to determine subject location and orientation when both camera and subject move relative to the scene, For. Sci. Int. 331 (2022) 111145.

[15] D. Seckiner, X. Mallett, C. Roux, D. Meuwly, P. Maynard, Forensic image analysis – CCTV distortion and artefacts, Forensic Sci. Int. 285 (2018) 77–85.

[16] Scientific Working Group on Digital Evidence (SWGDE), "SWGDE Best Practices for the Forensic Use of Photogrammetry," Version 1.2 (January 13 2022) (2022) [PDF].

[17] Organization of Scientific Area Committees for Forensic Science (OSAC), Standard Guide for Forensic Photogrammetry (OSAC 2021–S–0037, Registry version), added to OSAC Registry 04/04/2023.

[18] Scientific Working Group on Digital Evidence (SWGDE), "SWGDE Guidelines for the Digital Imaging of Footwear and Tire Impressions," Version 1.0 (April 25 2018) (2018).

[19] T. Terpstra, S. Miller, A. Hashemian, An evaluation of two methodologies for lens distortion removal when exif data is unavailable, SAE Technical Paper (2017) 2017-01-1422.

[20] Q. Sun, W.X. Wang, J. Xu, L. Wang, H. Zhang, J. Yu, T. Su, X. Zhang, Camera self-calibration with lens distortion, Optik 127 (2016) 4506–4513.

[21] J. Rong, S. Huang, Z. Shang, X. Ying, Radial lens distortion correction using convolutional neural networks trained with synthesized images, Lect. Notes Comput. Sci 10113 (2017) 35–49.

[22] L. Alvarez, L. Gómez, J.R. Sendra, An algebraic approach to lens distortion by line rectification, J. Math. Imag. Vision 35 (2009) 36–50.

[23] M. Alemán-Flores, L. Alvarez, L. Gomez, D. Santana-Cedrés, Automatic lens distortion correction using one-parameter division models, IPOL 4 (2014) 327–343.

[24] C. Brauer-Burchardt, K. Voss, A new algorithm to correct fish-eye- and strong wide-angle-lens-distortion from single images, Proc. 2001 Int. Conf. Image Processing 1 (2001) 225–228.

[25] D. Claus, A.W., Fitzgibbon, A rational function lens distortion model for general cameras, 2005 IEEE Comp. Soc. Conf. Comp. Vision Pattern Recognition 1, pp. 213–219.

[26] A. W. Fitzgibbon, Simultaneous linear estimation of multiple view geometry and Lens Distortion," Proc. 2001 IEEE Comp. Soc. Conf. Comp. Vision Pattern Recognition, 1 (2001) I-I.

[27] D.G. Bailey, A new approach to lens distortion correction,, Proc. Int. Conf. Image Vision Comp. New Zealand (2002) 59–64.

[28] J. Wang, F. Shi, J. Zhang, Y. Liu, A new calibration model of camera lens distortion, Pattern Recogn. 41 (2008) 607–615.

[29] L. Alvarez, L. Gómez, J.R. Sendra, Accurate depth dependent lens distortion models: an application to planar view scenarios, J. Math. Imaging Vision 39 (2011) 75–85.

[30] P. Ranganathan, E. Olson, Gaussian process for lens distortion modeling,, Int. Conf. Intelligent Robots Syst. (2012) 3620–3625.

[31] R. Cucchiara, C. Grana, A. Prati, R. Vezzani, A Hough Transform-based method for radial lens distortion correction, Proc. 12th Int. Conf. Image Analysis Processing (2003) 182–187.

[32] R. Sagawa, M. Takatsuji, T. Echigo, Y. Yagi, Calibration of lens distortion by structured-light scanning, IEEE/RSJ Int Conf. Intelligent Robots Syst. 2005 (2005) 832–837.

[33] S. Van der Jeught, J. Buytaert, J. Dirckx, Real-time geometric lens distortion correction using a graphics processing unit, Optical Eng. 5 (2012) 027002.

[34] D. Santana-Cedrés, L. Gómez, M. Alemán-Flores, A. Salgado, J. Esclarin, L. Mazorra, L. Alvarez, An iterative optimization algorithm for lens distortion correction using two-parameter models, IPOL 6 (2015) 326–364.

[35] D. Santana-Cedrés, L. Gomez, M. Alemán-Flores, A. Salgado, J. Esclarín, L. Mazorra, Estimation of the lens distortion model by minimizing a line reprojection error, IEEE Sensors J. 17 (2017) 2848–2855.

[36] W. Yu, Y. Chung, An embedded camera lens distortion correction method for mobile computing applications, IEEE Int Conf. Consumer Electronics 49 (2003) (2003) 400–401.

[37] T. Rahman, N. Krouglicof, An efficient camera calibration technique offering robustness and accuracy over a wide range of lens distortion,, IEEE Trans. Image Processing 21 (2012) 626–637.

[38] T. Terpstra, A. Hashemian, R. Gillihan, E. King, S. Miller, W. Neale, Accuracies in single image camera matching photogrammetry, SAE Technical Paper (2021).

[39] Z. Zhang, A flexible new technique for camera calibration, IEEE Trans. Pattern Anal. Mach. Intell. 22 (2000) 1330–1334.

[40] Adobe, Correct image distortion and noise, Photoshop. https://helpx.adobe.com/ca/photoshop/using/correcting-image-distortion-noise.html (accessed 20 October 2025).

[41] S. Chen, H. Jin, J. Chien, E. Chan, D. Goldman, Adobe Camera Model Technical Report, Adobe Systems Inc. (2010),https://download.macromedia.com/pub/labs/lensprofile_creator/lensprofile_creator_cameramodel.pdf.

[42] Photomodeler Technologies, Photomodeler Online user manual. https://www.photomodeler.com/downloads/OnlineHelp/index.html (accessed 23 October 2025).

[43] R. Rofallski, T. Luhmann, An efficient solution to ray tracing problems in multimedia photogrammetry for flat refractive interfaces, PFG, J. Photogramm. Remote Sens. Geoinf. Sci. 90 (2022) 37–54.

[44] V. Adobe, | Resizing images in Photoshop, in Adobe Photoshop help, Adobe (2019) 260–262.

[45] K. Mancini, J. Sidoriak, Digital Photography, in: Fundamentals of Forensic Photography, Routledge, New York, NY, (2017) 40–56.

[46] A. Dey, P.K. Rao, D. Rawtani, Forensic Photography, in: D. Rawtani, C.M. Hussain (Eds.), Modern Forensic Tools and Devices, (2023) 315-334.
[47] RealSense Inc, D415, https://www.realsenseai.com/products/stereo-depth-camera-d415/ (accessed Oct. 2, 2025).
[48] M. Servi, A. Profili, R. Furferi, Y. Volpe, Comparative evaluation of Intel RealSense D415, D435I, D455, and Microsoft Azure Kinect DK sensors for 3D vision applications, IEEE Access 12 (2024) 111311–111321.